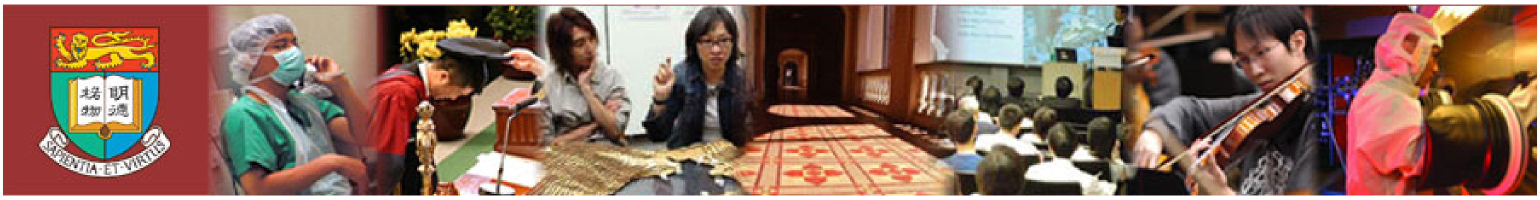

Auxiliary Circuits for Power Flow Control in Multifrequency Wireless Power Transfer Systems With Multiple Receivers

Wenxing Zhong, *Member, IEEE*, and S. Y. R. Hui, *Fellow, IEEE*

***Abstract*—This paper describes a technique for multifrequency wireless power transfer systems in which the wireless power can be transmitted through the wireless power transfer channel or channels from the transmitter to the targeted loads with receiver coils specifically tuned for energy reception. Auxiliary circuits comprising bandpass and/or bandstop circuits are proposed for incorporation into the receiver circuits and optional relay circuits so as to facilitate the selection and enhancement of the wireless power transfer to the designated load without causing significant cross interference due to the use of multifrequency wireless power flow control. A unique feature of this technique is that the nontargeted receiver will automatically act as a relay resonator to enhance 1) magnetic coupling, and thus, 2) the power transfer between the power transmitter and the targeted receiver. A second novel feature is that the chosen operating frequencies for the tuned receivers need not be widely apart because the auxiliary circuits consist of bandpass and/or bandstop filters to reduce any cross interference from the nontargeted frequency. The proposed technique has been practically verified in experimental prototype.**

***Index Terms*—Multifrequency WPT, multiple receivers, wireless power transfer (WPT).**

I. Introduction

Wireless power transfer (WPT) technology has reemerged as a viable technology for domestic and industrial applications. Several review papers [1]–[4] have listed many relevant references dating back to the work of Tesla reported in the last century [5]. Recently, multiple-frequency wireless power transmission has been proposed as a means to enhance WPT [6]–[9]. In [6], multiresonant tanks are used at the transmitter and receiver to amplify and extract power at multiple frequencies. The power transfer is carried out at a fundamental frequency of 25 kHz and the third harmonic of 75 kHz. Power transfer is spread over more than one frequency so as to increase the power transfer. Single-frequency receivers are used to receiver power sent at different frequencies. For example, if the targeted receiver is tuned at 25 kHz, then transmitting power at 25 kHz will theoretically transfer power to the receiver coil tuned at 25 kHz. The receiver coil tuned at 75 kHz will be the nontargeted receiver. A study on a WPT system with uncoupled receivers is reported in [10]. However, for near-field coupling based on one transmitter coil, it is likely that receivers are magnetically coupled to some extent. In fact, the coupling effects of three receivers powered by one transmitter coil are not negligible as reported in [11] and [12]. The general effects of multiple coils systems can be found in [13].

In [14], multiple receivers are used to control robotic swarms based on a transmitter operating at a fixed frequency. Such an approach is a conceptual advancement, but there is scope for further improvement in terms of the control of power flow. If multiple frequencies are used, wireless power can be transferred to a targeted group of mobile robots directly without affecting the nontargeted group. The use of multiple frequencies in WPT systems has several aspects that need special attention. Among them, one major limitation is that the residual power will be picked up by the nontargeted receiver unless the chosen frequencies are widely apart and/or the quality factors (Q-factor) of the resonators are very high (and thus very expensive). The choice of widely apart frequencies also leads to considerable technical and cost constraints on the power transmitter design and the coil resonator design.

In this paper, a novel method [15] that provides selective and enhanced power flow in WPT systems with multiple receivers is presented. Auxiliary circuits are introduced in the receiver circuits (and relay circuits if applicable) so as to ensure proper frequency selective wireless power flow to the appropriate targeted receivers, with the pickup power by the nontargeted receivers substantially reduced even if the chosen tuned frequencies for different receivers are not widely apart. An analysis is included to explain the operating principle, and experimental results are provided to confirm the validity of the proposal.

II. Analysis of WPT Systems With Multiple Receivers

Before the new method is explained in detail, it is necessary to understand some key issues of using multifrequency for WPT. For the WPT system shown in Fig. 1, the transmitter is assumed to be able to operate at more than one frequency. For simplicity, it is assumed that the WPT system can be operated at two operating frequencies, namely f_1 and f_2, and that it has two receivers tuned at f_1 and f_2, respectively, for receiving power. In this way, the power flow of each receiver can be controlled separately by controlling the frequency of the power source.

Manuscript received June 3, 2014; revised September 19, 2014; accepted November 10, 2014. Date of publication November 21, 2014; date of current version May 22, 2015. This work was supported by the Hong Kong Research Grant Council under Project GRF HKU 712913E, and by the University of Hong Kong. Recommended for publication by Associate Editor B. Lehman.

W. Zhong is with the Department of Electrical and Electronic Engineering, The University of Hong Kong, Hong Kong (e-mail: wenxingzhong@gmail.com).

S. Y. R. Hui is with the Department of Electrical and Electronic Engineering, The University of Hong Kong, Hong Kong, and also with Imperial College London, London SW7 2AZ, U.K. (e-mail: ronhui@eee.hku.hk).

Color versions of one or more of the figures in this paper are available online at http://ieeexplore.ieee.org.

Digital Object Identifier 10.1109/TPEL.2014.2373381

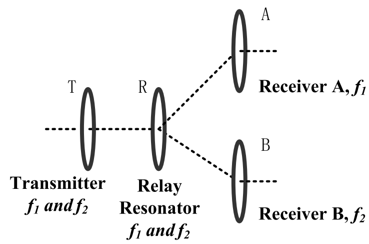

Fig. 1. Schematic of a WPT system with two operating frequencies each of which is applied to one receiver and one load.

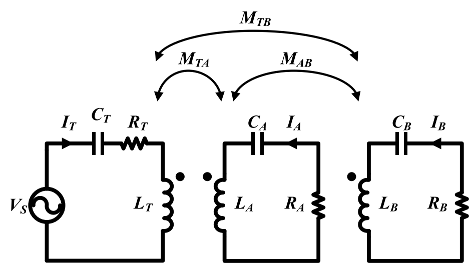

Fig. 2. Lumped circuit model of the system shown in Fig. 1 without the relay resonator.

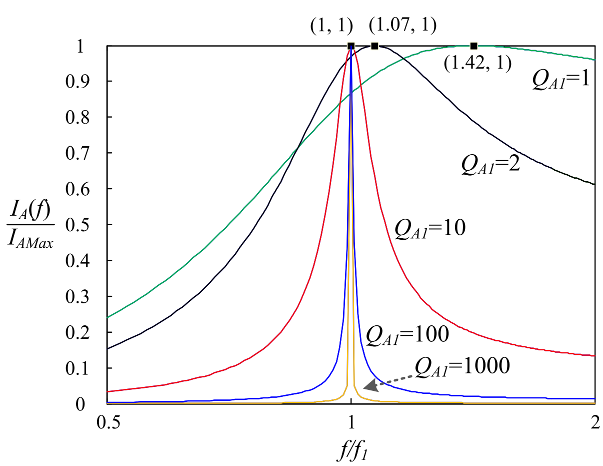

Fig. 3. Current variations according to the operating frequency under different Q-factors.

The use of the relay resonator in Fig. 1 is to increase the transmission distance. Its presence does not affect the basic principle of the proposed method. For simplicity, the relay resonator is not included in this part of the analysis. The lumped circuit model of the two-receiver system with series compensation is shown in Fig. 2, and its circuit equations are listed below for one operating frequency

$$(R_T + jX_T)\mathbf{I_T} + j\omega M_{TA}\mathbf{I_A} + j\omega M_{TB}\mathbf{I_B} = \mathbf{V_S} \quad (1)$$

$$j\omega M_{TA}\mathbf{I_T} + (R_A + jX_A)\mathbf{I_A} + j\omega M_{AB}\mathbf{I_B} = 0 \quad (2)$$

$$j\omega M_{TB}\mathbf{I_T} + j\omega M_{AB}\mathbf{I_A} + (R_B + jX_B)\mathbf{I_B} = 0 \quad (3)$$

where $\omega = 2\pi f$; R_T is the total resistance in the transmitter loop, which includes the source resistance of the source and the parasitic resistance of the inductor and the capacitor; R_A and R_B are the resistance in two receiver coils A and B, respectively,

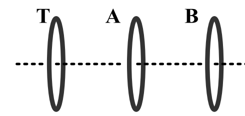

Fig. 4. Physical arrangement of a practical WPT system with three coaxial resonators.

which include the "load" resistance (R_{LN}) (assuming pure resistive load in the analysis) and the "parasitic" resistance (R_{PN}) of the inductors and the capacitors for $N = A$ or *B*; and X_N is the reactance in loop *N*, which equals to $\omega L_N - 1/(\omega C_N)$. For example, for Receiver-A, $R_A = R_{PA} + R_{LA}$. $\mathbf{V_S}$ is the voltage vector of the power source that drives the transmitter coil. $\mathbf{I_T}$, $\mathbf{I_A}$, and $\mathbf{I_B}$ are the current vectors of the transmitter coil, receiver-A, and receiver-B, respectively.

The main power transfer path for each receiver is from the transmitter to the receiver directly. If the receiver is tuned at the operating frequency of the transmitter, such receiver is called the "targeted" receiver. Otherwise, it is called the "nontargeted" receiver. Assume that Receiver-A is tuned at f_1, and Receiver-B is tuned at f_2. Since Receiver-A and Receiver-B consist of resonators, they are also referred as Resonator-A and Resonator-B when the operating principle is explained in this paper.

In the example of Fig. 1, the main power transfer path for frequency f_1 is T-A because Receiver-A is the targeted receiver, and the power transfer path T-B-A is traditionally blocked for the power flow of f_1 in order to reduce the power reception in Resonator-B at f_1. Thus, the example in Fig. 1 can be considered as the combination of two two-resonator systems. In the past, Tesla proved that the resonant frequency of the receiver should be equal to the operating frequency in order to obtain high power transfer efficiency (PTE) for a two-resonator system [1]. Therefore, the resonant frequency of Resonator-A should be equal to f_1, and the resonant frequency of Resonator-B should equal to f_2

$$\omega_1 = \frac{1}{\sqrt{L_A C_A}} \text{ and } \omega_2 = \frac{1}{\sqrt{L_B C_B}}. \quad (4)$$

For each receiver that behaves like a tuned resonator, it also acts like a bandpass filter. Take Resonator-A as an example. Its current $I_A(f)$ can be expressed as

$$\begin{aligned} I_A(f) &= \frac{\omega M_{TA} I_T}{\sqrt{R_A^2 + X_A^2}} = \frac{\omega M_{TA} I_T}{\sqrt{R_A^2 + \left(\omega L_A - \frac{1}{\omega C_A}\right)^2}} \\ &= \frac{\omega M_{TA} I_T}{\sqrt{\frac{\omega_1^2 L_A^2}{Q_{A1}^2} + \omega^2 L_A^2 \left(1 - \frac{\omega_1^2}{\omega^2}\right)^2}} \\ &= \frac{M_{TA} I_T}{L_A \sqrt{\frac{\omega_1^2}{\omega^2 Q_{A1}^2} + \left(1 - \frac{\omega_1^2}{\omega^2}\right)^2}} \end{aligned} \quad (5)$$

where $\omega_1 = 1/\sqrt{L_A C_A}$; $Q_{A1} = \omega_1 L_A / R_A$ is the Q-factor of the Resonator-A at the resonant frequency. Fig. 3 shows the

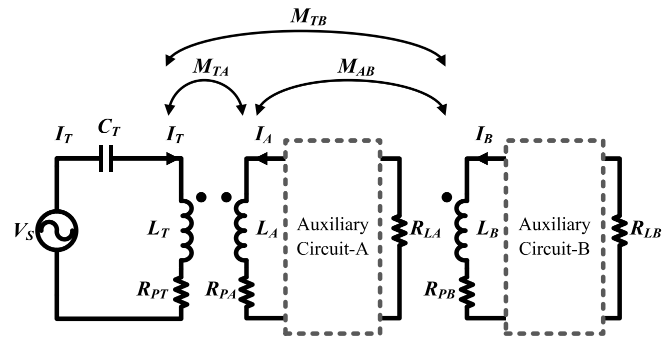

Fig. 5. Circuit diagram of a system with auxiliary circuits and utilizing indirect power paths.

per-unit current profiles of the resonator as functions of the operating frequency f and the Q-factor Q_{A1}. It is important to note that the shape of the current–frequency characteristic depends on the Q-factor of the coil resonator. A sharp current–frequency characteristic is only possible if the Q-factor is very high (say $\mathrm{Q} = 1000$, which is difficult to achieve at low cost). In general, this current–frequency characteristic curve exhibits a bell-shape with its peak occurring at or near the resonant frequency. Therefore, if the tuned resonant frequency of the nontarget receiver is close to that of the target receiver, the nontarget receiver will also pick up some current and, therefore, some power unintentionally. This unintentional power pickup by the nontarget receiver is called "cross interference" in this paper. On the other hand, if the Q-factor is very high and the current–frequency curve is very sharp, a slight deviation of the operating frequency due to various reasons such as temperature drift of component values may cause the power transfer to reduce drastically.

It is important to note in the traditional approach [6]–[9] that the nontargeted receiver resonator is normally *not used* because it is not the targeted receiver. In this proposed method, the nontargeted receiver is *used* as a relay resonator to enhance the magnetic coupling and, therefore, power transfer between the transmitter coil and the targeted receiver coil. This novel feature of this patent-pending technique [15] needs special attention. It has been demonstrated that a three-coil WPT system (with one relay coil-resonator) can achieve higher energy efficiency than the two-coil counterpart under some design conditions [16], [17]. So the proposed method and auxiliary circuits will add advantages to the WPT systems with multiple receivers because the nontargeted receiver (which is not used traditionally) will be used as a relay resonator.

From (2) and (3), the ratio between the currents in Resonator-A and Resonator-B can be expressed as

$$\frac{\mathbf{I_2}}{\mathbf{I_3}} = \frac{M_{TA}R_B + j(M_{TA}X_B - \omega M_{TB}M_{AB})}{M_{TB}R_A + j(M_{TB}X_A - \omega M_{TA}M_{AB})}. \tag{6}$$

Since the proposed method allows not only the WPT at a single frequency to the targeted receiver but also multiple frequencies to multiple targeted receivers, the following explanations are not restricted to the single-frequency operation.

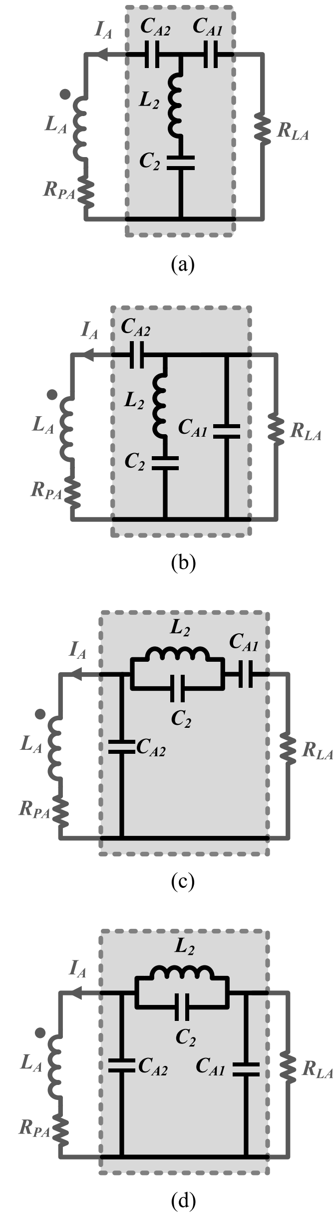

Fig. 6. Circuit diagrams of the four proposed L–C networks for Resonator-A. (a) Shunt resonant circuit (L_2 and C_2) to bypass the current of nontargeted frequency (f_2) for series-connected load (RLA targeted for receiving power at frequency f_1). (b) Shunt resonant circuit (L_2 and C_2) to bypass the current of nontargeted frequency (f_2) for parallel-connected load (RLA targeted for receiving power at frequency f_1). (c) Parallel resonant circuit (L_2 and C_2) to block the current of nontargeted frequency (f_2) for series-connected load (RLA targeted for receiving power at frequency f_1). (d) Parallel resonant circuit (L_2 and C_2) to block the current of nontargeted frequency (f_2) for parallel-connected load (RLA targeted for receiving power at frequency f_1).

In order to quantify the cross interference introduced by the untargeted current in a targeted receiver, an index (δ) equaling to the ratio of the maximum power caused by the untargeted current harmonic and the minimum targeted output power generated by the targeted current component in the receiver. (Note: Such minimum targeted output power can be a predetermined value). For example, if the rated output power of a receiver is 5 W, and the untargeted power is to be limited to be less than 5% of the targeted power even when the minimum targeted output power

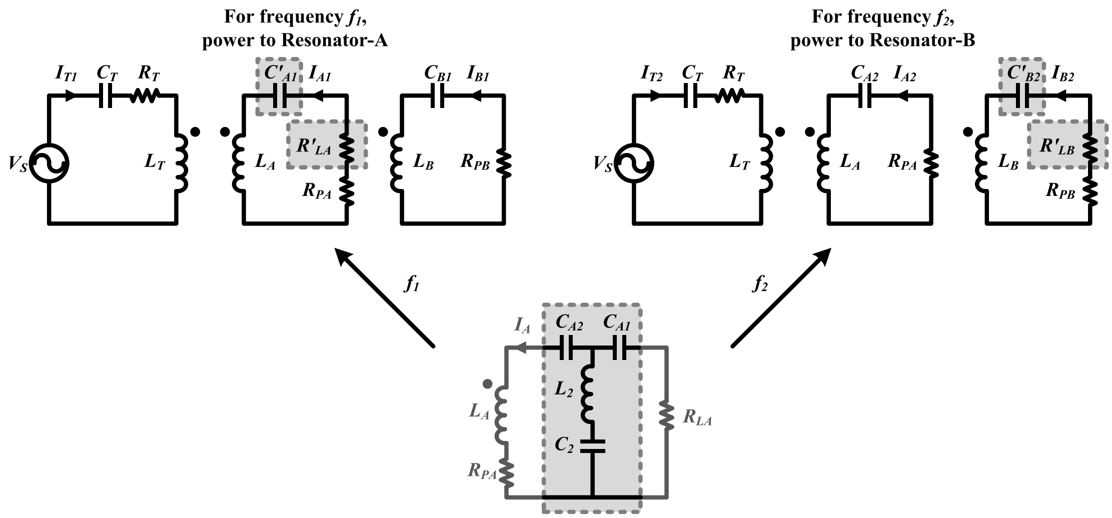

Fig. 7. Two operating conditions of the auxiliary circuit in Resonator-A (the couplings are not shown for simplicity).

is set at 0.1 of the rated power, then in this case, the minimum targeted output power of this receiver is 0.5 W. Assuming the general case of transmitting power at both of the frequencies f_1 and f_2 in Fig. 1 for Resonator-A, the index is

$$\delta_A = \frac{P_{A2\max}}{P_{A1\min}} \tag{7}$$

where $P_{A2\max}$ is the maximum untargeted power caused by the untargeted current of f_2, and $P_{A1\min}$ is the minimum targeted power caused by the targeted current of f_1 in the equivalent load R_A.

Similarly, for Resonator-B

$$\delta_B = \frac{P_{B1\max}}{P_{B2\min}} \tag{8}$$

where $P_{B1\max}$ is the maximum untargeted power caused by the untargeted current of f_1, and $P_{B2\min}$ is the minimum targeted power caused by the targeted current of f_2 in the equivalent load R_B. It can be seen from (7) and (8) that a large index implies that the cross interference is significant and the situation is not desirable.

By utilizing (6), (7) and (8) can be rewritten as

$$\delta_A = \frac{P_{B2\max}R_{LA}}{P_{A1\min}R_{LB}} \cdot \frac{M_{TA}^2 R_B^2 + \omega_2^2 M_{TB}^2 M_{AB}^2}{M_{TB}^2 R_A^2 + (M_{TB}L_A(\omega_2 - \omega_1^2/\omega_2) - \omega_2 M_{TA}M_{AB})^2} \tag{9}$$

$$\delta_B = \frac{P_{A1\max}R_{LB}}{P_{B2\min}R_{LA}} \cdot \frac{M_{TB}^2 R_A^2 + \omega_1^2 M_{TA}^2 M_{AB}^2}{M_{TA}^2 R_B^2 + (M_{TA}L_B(\omega_1 - \omega_2^2/\omega_1) - \omega_1 M_{TB}M_{AB})^2}. \tag{10}$$

Here is one design example with two receiver coils with resonant frequency close to each other ($f_1 = 600$ kHz; $f_2 = 500$ kHz). This example is used to illustrate the problems in a traditional setup with two close resonant frequencies. For the system shown in Fig. 4, the given parameters are: $L_A = L_B = 81.3\ \mu$H; $R_{PA} = R_{PB} = 0.85\ \Omega$; $M_{TA} = M_{AB} = 2.6624\ \mu$H; $M_{TB} = 0.49\ \mu$H; $\delta_A = 10\%$; $\delta_B = 10\%$; $P_{A1\max} = P_{B2\max} = 2.5$ W; and $P_{A1\min} = P_{B2\min} = 0.25$ W. The calculated values for the load resistance are $R_{LA} = 1.49\ \Omega$ and $R_{LB} = 1.24\ \Omega$ by solving (9) and (10). The load resistance values are small in order to increase the Q-factors of the receivers according to the previous analysis. From previous studies, there is an optimum value $R_{\rm opt}$ for the load resistance at which the maximum energy efficiency can be achieved. If the load resistance is much smaller than $R_{\rm opt}$, the energy efficiency of the system will be reduced.

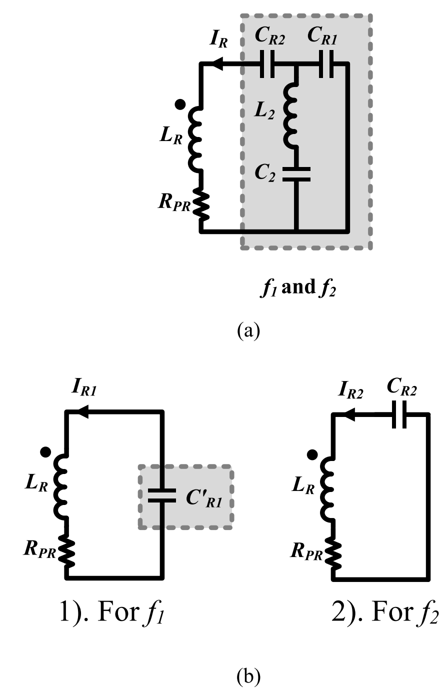

Fig. 8. (a) Auxiliary circuit in the relay resonator for both operating frequencies. (b) Equivalent circuits of the auxiliary circuit in the relay resonator.

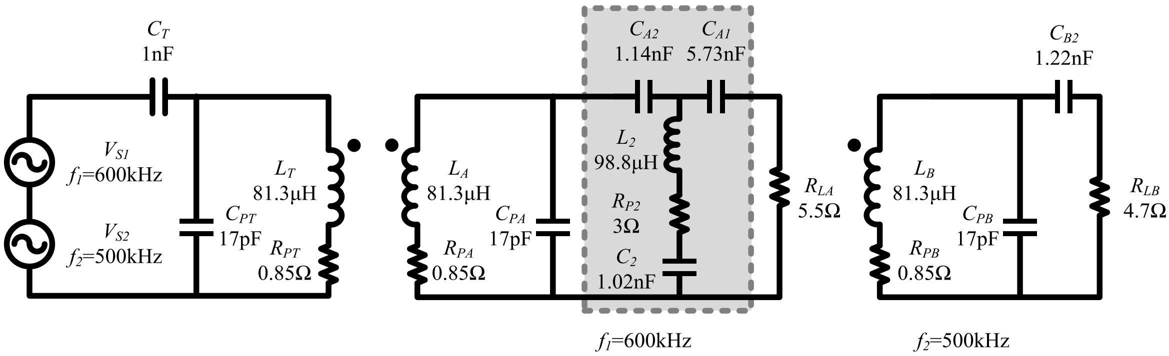

Fig. 9. Straight WPT system with auxiliary circuit in Resonator-A and optimized parameters.

TABLE I
COMPARISON BETWEEN CALCULATED AND EXPERIMENTAL RESULTS OF THE STRAIGHT WPT SYSTEM WITH AUXILIARY CIRCUIT AND WITHOUT AUXILIARY CIRCUIT

			With Auxiliary Circuit			Without Auxiliary Circuit		
	P_A at 600 kHz	P_B at 500 kHz	δ_A	δ_B	η	δ_A	δ_B	η
Calculated	2.5 W	2.5 W	0.1%	0.4%	**66.0%**	1%	1%	**50.1%**
	0.25 W	2.5 W	1.1%	0.04%	**59.9%**	10%	0.1%	**43.3%**
	2.5 W	0.25 W	0.01%	3.8%	**73.4%**	0.1%	10%	**59.5%**
Experiment	2.5 W	2.5 W	0.47%	0.23%	**59.7%**	1.87%	0.97%	**46.7%**
	0.25 W	2.5 W	7.2%	0.04%	**44.6%**	17.7%	0.09%	**37.1%**
	2.5 W	0.25 W	0.17%	4.2%	**72.6%**	0.16%	8.8%	**57.9%**

However, the small load resistance values might lead to low efficiency. In this case, the overall efficiency is 48.2%, while the possible maximum efficiency of the system is 59.6% if the load resistance values are optimized, which are $R_{LA} = 10.06\ \Omega$ and $R_{LB} = 1.76\ \Omega$. The load resistance and the operating frequencies could be further adjusted to obtain higher PTE, but there are always compromises to make between the frequency difference and the efficiency (decided by operating frequencies and load resistance values). Also, it should be noted that (9) and (10) are only valid for a narrow frequency range in which the ac resistance of the resonator can be considered as constant.

In spite of the difficulty to achieve high efficiency, the drawbacks of the traditional method also include: 1) it cannot remove the undesired current substantially; 2) the indirect power transfer paths (for example T-A-B for Resonator-B in the system in Fig. 4) are not utilized, which is a waste of the power transfer capability of the system; 3) the interferences are highly sensitive to the resonant frequencies of the resonators (i.e., the inductance and capacitance values of the resonator) due to the high Q-factors. This will be demonstrated with experimental measurements.

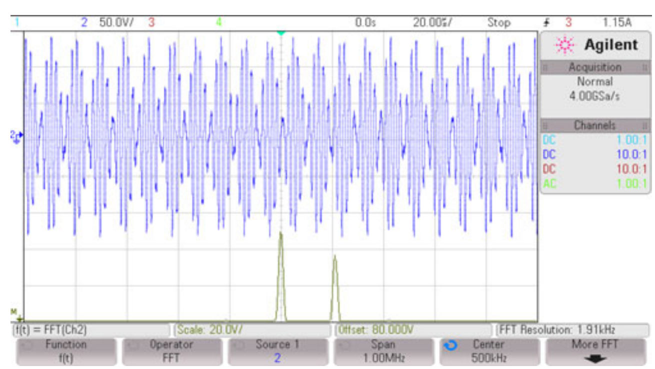

Fig. 10. Input voltage and its FFT (50 V/div for the waveform and 20 V/div for the FFT).

III. NEW AUXILIARY CIRCUITS FOR SELECTING AND ENHANCING WPT

The essence of the proposed method is to utilize the nontargeted coil as a relay resonator in order to enhance the magnetic coupling and power transfer between the transmitter coil and the targeted receiver coil. There are many practical applications in which indirect power paths should be utilized in order to raise the power transfer capability. For example, for the system shown in Fig. 4, the direct path for Resonator-B is T-B and the indirect power path is T-A-B. The PTE of the system will be much higher if both of the direct and indirect paths are used. It has been demonstrated in [13] and [17] that the cross-coupling (or indirect) power transfer paths can be utilized to further increase the capacity of power transfer.

A. Auxiliary Circuits for the Receivers

In order to utilize indirect power paths, new auxiliary circuits are proposed as shown in Fig. 5. Assuming the tuned resonant frequencies of Resonator-A and Resonator-B are f_1 and f_2, respectively, the functions of auxiliary circuit for the receivers are first explained.

TABLE II
COMPARISON BETWEEN THE INTERFERENCES OF THE STRAIGHT WPT SYSTEM WITH AUXILIARY CIRCUIT AND WITHOUT AUXILIARY CIRCUIT AND $P_A = P_B = 2.5$ W

	With Auxiliary Circuit	Without Auxiliary Circuit
V_{RLA}	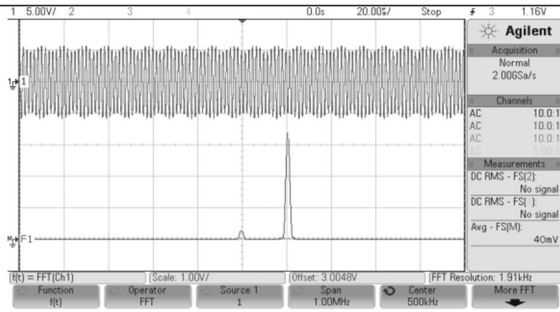 $\delta_A = 0.47\%$ (5V/div for the waveform and 1V/div for the FFT)	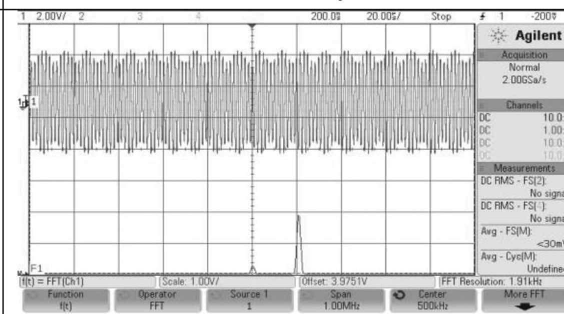 $\delta_A = 1.87\%$ (2V/div for the waveform and 1V/div for the FFT)
V_{RLB}	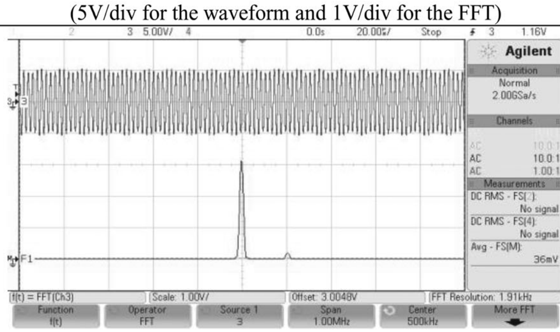 $\delta_B = 0.23\%$ (5V/div for the waveform and 1V/div for the FFT)	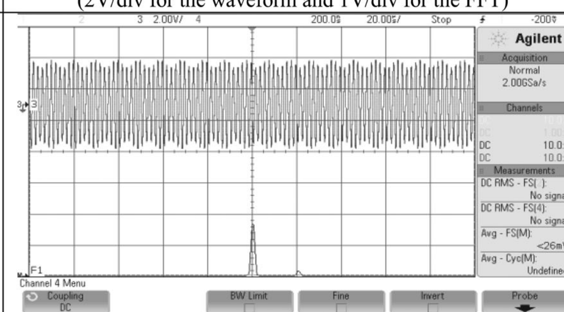 $\delta_B = 0.97\%$ (2V/div for the waveform and 1V/div for the FFT)

Four types of auxiliary circuits are proposed as shown in Fig. 6 to cover the use of 1) shunt resonant branch to bypass and 2) parallel resonant branch to block the power flow of nontargeted frequency for series-connected and parallel-connected loads in the receivers. The shunt and parallel auxiliary circuits described in this section are of the simplest form adequate for acting as bypass filters and blocking filters, respectively, (as shown in the experimental results). Their typical voltage and current ratings are similar to those of the original circuits. In this paper, the concept of using the bypass filters and blocking filters is described in a general sense. Other forms of filters can be explored if necessary. In the traditional approach, a receiver consists of a resonant inductor (*L*), a resonant capacitor (*C*), and the load can be connected in series with the *L* and *C* or in parallel with *C*.

1) Design Methodology for the Shunt Resonant Circuit Branch to Bypass Current of Nontargeted Frequency for a Series-Connected Load [see Fig. 6(a)]: Fig. 6(a) shows the one proposed circuit including the auxiliary circuit (enclosed in the dotted box) for the coil of Receiver-A. The coil inductance is L_A and the coil resistance is R_{PA}. For Receiver-A, f_1 is its targeted frequency and f_2 is its nontargeted frequency. In the auxiliary circuit of Receiver-A, the resonant branch comprising L_2 and C_2 is designed to resonate at the frequency f_2 so that it acts as a shunt circuit to short circuit (bypass) the current caused by power transmission at frequency f_2. In this way, the current of the nontargeted frequency will circulate within a close loop. This special phenomenon offers two advantageous functions.

1) First, if the transmitter is transmitting power at f_2, this current loop of f_2 will act as a relay loop resonator to enhance the magnetic coupling and power transfer between the transmitter and Receiver-B (which has a targeted frequency of f_2). Consequently, it provides an extra power flow path from the transmitter to Receiver-B.
2) Second, the circulating current of frequency f_2 in the closed loop $R_{PA} - L_A - C_{A2} - L_2 - C_2$ will not affect the load R_{LA} (which has its targeted frequency of f_1).

Note that the two capacitors C_{A1} and C_{A2} are used to form parts of the resonant circuit for the resonant frequency f_1 for the Receiver-A and that the shunt resonant circuit is connected between the ground and the joint of C_{A1} and C_{A2}.

In order to design the circuit of Fig. 6(a) as Receiver-A, it is necessary for its resonant frequency to be tuned at or near the targeted frequency f_1. With the help of the equivalent circuit in Fig. 7, the designs of the resonant inductors and capacitors can be achieved. Fig. 7 shows the two equivalent circuits of Fig. 4—the one on the left for frequency f_1 and the one on the right for frequency f_2. At an operating frequency of f_1, it is necessary to design the equivalent circuit of Receiver-A in Fig. 7 so that it receives power at the targeted frequency of f_1. At f_1, the total impedance of the auxiliary circuit connected with the load R_{LA} will be equivalent to that of a capacitance C'_{A1} in series

TABLE III
COMPARISON BETWEEN THE INTERFERENCES OF THE STRAIGHT WPT SYSTEM WITH AUXILIARY CIRCUIT AND WITHOUT AUXILIARY CIRCUIT AND $P_A = 2.5$ W; $P_B = 0.25$ W

	With Auxiliary Circuit	Without Auxiliary Circuit
V_{RLA}	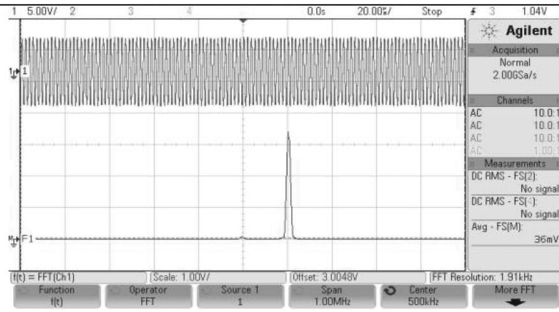 $\delta_A = 0.17\%$ (5V/div for the waveform and 1V/div for the FFT)	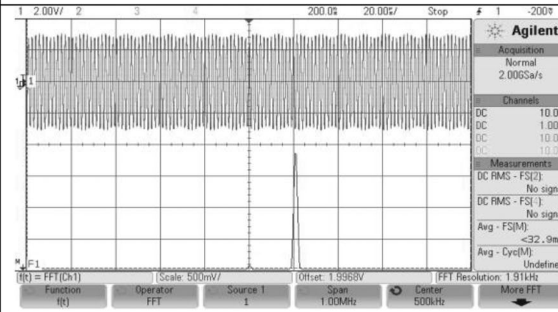 $\delta_A = 0.16\%$ (2V/div for the waveform and 0.5V/div for the FFT)
V_{RLB}	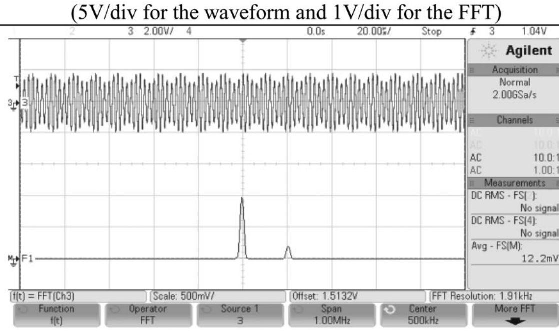 $\delta_B = 4.2\%$ (2V/div for the waveform and 0.5V/div for the FFT)	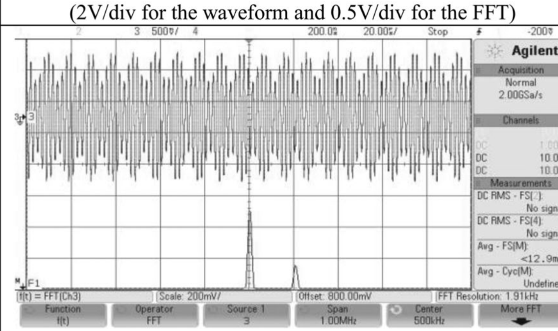 $\delta_B = 8.8\%$ (0.5V/div for the waveform and 0.2V/div for the FFT)

with an equivalent load resistance R'_{LA}. The total impedance of Receiver-A can be expressed as

$$Z_A = R_{PA} + \frac{X_2^2 R_{LA}}{R_{LA}^2 + \left(X_2 - \frac{1}{\omega_1 C_{A1}}\right)^2} + j\left(\omega_1 L_A + \frac{X_2\left(R_{LA}^2 + \frac{1}{\omega_1^2 C_{A1}^2} - \frac{X_2}{\omega_1 C_{A1}}\right)}{R_{LA}^2 + \left(X_2 - \frac{1}{\omega_1 C_{A1}}\right)^2} - \frac{1}{\omega_1 C_{A2}}\right) \quad (11)$$

where $X_2 = \omega_1 L_2 - \frac{1}{\omega_1 C_2}$. Therefore, the equivalent load resistance (R'_{LA}) and equivalent capacitance (C'_{A1}) can be expressed as

$$R'_{LA} = \frac{X_2^2 R_{LA}}{R_{LA}^2 + \left(X_2 - \frac{1}{\omega_1 C_{A1}}\right)^2} \quad (12)$$

$$-\frac{1}{\omega_1 C'_{A1}} = \frac{X_2\left(R_{LA}^2 + \frac{1}{\omega_1^2 C_{A1}^2} - \frac{X_2}{\omega_1 C_{A1}}\right)}{R_{LA}^2 + \left(X_2 - \frac{1}{\omega_1 C_{A1}}\right)^2} - \frac{1}{\omega_1 C_{A2}}. \quad (13)$$

From (13), the equivalent capacitor C'_{A1} can be calculated. Then the inductance L_A and C'_{A1} can be designed so that the $L_A - C'_{A1}$ branch forms a resonant tank at or near its targeted resonant frequency of f_1

$$f_1 \approx \frac{1}{2\pi\sqrt{L_A C'_{A1}}}. \quad (14)$$

At f_2, L_2 and C_2 will bypass the current of f_2; therefore, Resonator-A is equivalent to a repeater resonator with C_{A2} as its compensating capacitor as shown in the equivalent circuit on the right of Fig. 7.

2) Design Methodology for the Auxiliary Circuit in Fig. 6(b): The design principle applies previously to Fig. 6(a) can be applied to Fig. 6(b). The only difference is that in Fig. 6(b), the load is connected across the capacitor C_{A1}. Again, L_2 and C_2 are designed to form a bypass resonant tank for the nontargeted frequency f_2. Then the circuit of Fig. 6(b) can be transformed into the equivalent form of Fig. 7. Afterwards, the equations of the equivalent load R'_{LA} and the equivalent capacitor C'_{A1} specific for the circuit of Fig. 6(b) can be derived. From these equations, C'_{A1} can be chosen with L_A to form a resonant tank at a frequency at or near its targeted frequency according to (14).

3) Design Methodology for the Auxiliary Circuit in Fig. 6(c) and (d): Unlike the auxiliary circuits of Fig. 6(a) and (b) that use the series-connected L_2 and C_2 as a bandpass filter to short the current of the nontargeted frequency, those in Fig. 6(c) and (d) use the parallel-connected L_2 and C_2 as a bandstop filter to block the current of the nontargeted frequency of f_2 from Receiver-A. The circuit in Fig. 6(c) has the load R_{LA} connected in series with the capacitor C_{A1}, while that in Fig. 6(d) has the load R_{LA} connected in parallel with C_{A1}. Regardless of the series- or parallel-connected load, the design methodology of the auxiliary circuits of Fig. 6(c) and (d) follow similar principle previously described. The auxiliary circuits can be transformed into the

TABLE IV
COMPARISON BETWEEN THE INTERFERENCES OF THE STRAIGHT WPT SYSTEM WITH AUXILIARY CIRCUIT AND WITHOUT AUXILIARY CIRCUIT AND $P_A = 0.25$ W; $P_B = 2.5$ W

	With Auxiliary Circuit	Without Auxiliary Circuit
V_{RLA}	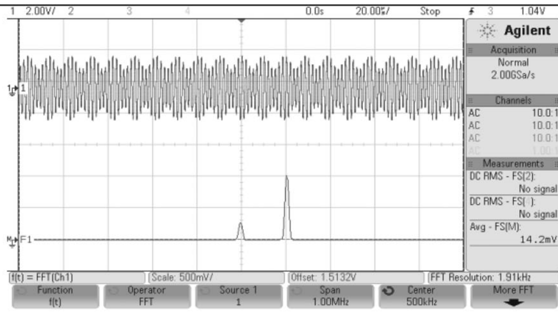 $\delta_A = 7.2\%$ (2V/div for the waveform and 0.5V/div for the FFT)	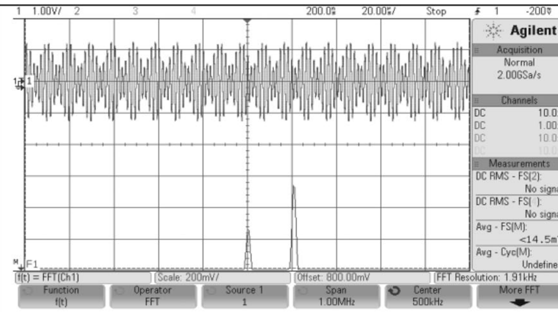 $\delta_A = 17.7\%$ (1V/div for the waveform and 0.2V/div for the FFT)
V_{RLB}	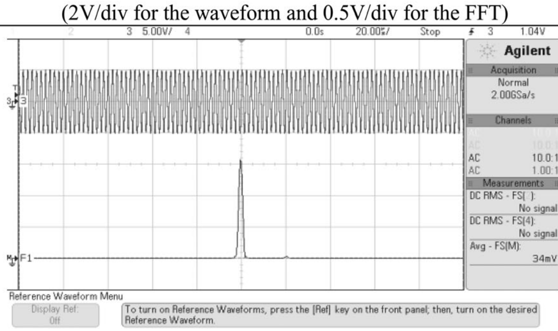 $\delta_B = 0.04\%$ (5V/div for the waveform and 1V/div for the FFT)	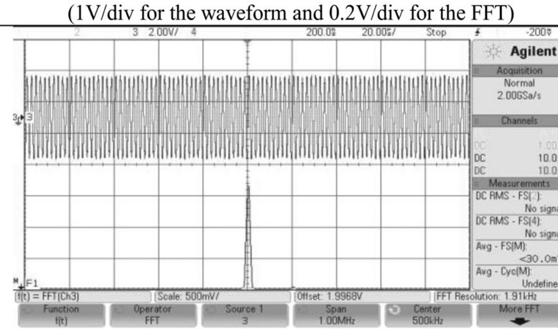 $\delta_B = 0.09\%$ (2V/div for the waveform and 0.5V/div for the FFT)

equivalent forms of Fig. 7. Then the equivalent load R'_{LA} and equivalent capacitance C'_{A1} equations can be derived. L_A and C'_{A1} can be designed together to satisfy (14).

The design methodology for the Receiver-B is the same as that for the Receiver-A, except that the targeted-frequency is f_2 instead of f_1.

B. Auxiliary Circuit as a Relay Resonator

By replacing the loads in the proposed auxiliary circuits in Fig. 6 with a short circuit, each of the auxiliary circuits will become a relay resonator. Such resonators should be tuned to the multiple frequencies if they are used generally as relay resonators. Fig. 8(a) shows an example of a relay resonator which can operate with more than one tuned frequencies. In this example, it is tuned to work at f_1 and f_2. The two equivalent circuits for f_1 and f_2 are shown in Fig. 8(b). At f_1, the whole auxiliary circuit indicated in the dotted box shows a capacitive impedance which can compensate L_R and form an *L–C* resonant tank at f_1. At f_2, L_2 and C_2 will be resonant and form a short circuit to bypass C_{R1}, thereby, L_R and C_{R2} form an *L–C* resonant tank at f_2.

IV. EXPERIMENTAL VERIFICATIONS

In order to demonstrate the principle of the proposed idea, a three-coil WPT system has been set up as shown in Fig. 4. The transmitter, Receiver-A, and Receiver-B are placed in a straight line in this example. For the straight system shown in Fig. 4, the indirect path T-A-B for Resonator-B is much more significant than the direct path T-B in terms of the PTE. Therefore, this indirect path should be utilized. But the indirect path T-B-A for Resonator-A has negligible effect since the direct path T-A is highly efficient. Generally, if the indirect path for one of the receivers (e.g., coil B) is important, it implies that the magnetic coupling between T-A (i.e., part of the path T-A-B) should be stronger than that between T-B (direct path). For Resonator-A, the indirect path T-B-A is weaker because the magnetic coupling between T-B (part of T-B-A) is already weaker than that between T-A (direct path). Therefore, the indirect path T-B-A has much less contribution for power transfer than the direct path T-A.

Based on the system in Fig. 4, one auxiliary circuit is used in Resonator-A has been set up. The parameters and the load resistance values are shown in the circuit diagram of the system in Fig. 9. The excitation voltage consisting of two frequencies (namely 500 and 600 kHz) is used to drive the transmitter coil. Table I lists the calculated and experimental results with and without the auxiliary circuit. From these results, the cross interference of the system with the proposed auxiliary circuit is largely reduced compared with that without the auxiliary circuit. With the rated output power, the PTE improvement is about 13% by applying the proposed auxiliary circuit.

Fig. 10 shows the waveform of the input voltage of the system and its fast Fourier transform (FFT) result. It is clear that the input voltage mainly includes two components 500 and 600 kHz.

Tables II–IV show the output voltage waveforms comparisons between the systems with and without the proposed auxiliary circuit.

V. Conclusion

The idea of using auxiliary circuits to select and enhance the power flow in wireless power systems with multiple receivers tuned at different receptive frequencies has been explained and experimentally demonstrated. Based on these practical measurements, it can be concluded that the proposed auxiliary circuits are suitable for WPT systems with multifrequency operation. The auxiliary circuits can reduce the cross interference from the power of the nontargeted frequency, and simultaneously improve the overall system energy efficiency. The proposed technique enables the development of new wireless power systems in which power flow control can be achieved by selecting the appropriate operating frequency of the transmitter circuit and the power flow can be directed to the targeted receiver, while the nontargeted receiver acts as a relay resonator to enhance the magnetic coupling and power transfer. This new concept has been verified with experiments.

References

[1] L. P. Wheeler, "Tesla's contribution to high frequency," *Elect. Eng.*, vol. 62, pp. 355–357, Aug. 1943.

[2] G. A. Covic and J. T. Boys, "Inductive power transfer," *Proc. IEEE*, vol. 101, no. 6, pp. 1276–1289, Jun. 2013.

[3] S. Y. R. Hui, "Planar wireless charging technology for portable electronic products and Qi," *Proc. IEEE*, vol. 101, no. 6, pp. 1290–1301, Jun. 2013.

[4] S. Y. R. Hui, W. X. Zhong, and C. K. Lee, "A critical review on recent progress of mid-range wireless power transfer," *IEEE Trans. Power Electron.*, vol. 29, no. 9, pp. 4500–4511, Sep. 2014.

[5] N. Tesla, "Apparatus for transmitting electrical energy," U.S. Patent 1 119 732, Dec. 1, 1914.

[6] Z. Pantic, K. Lee, and S. Lukic, "Inductive power transfer by means of multiple frequencies in the magnetic link," in *Proc. IEEE Energy Convers. Congr. Expo.*, Denver, CO, USA, Sep. 2013, pp. 2912–2919.

[7] D. Ahn and S. Hong, "Effect of coupling between multiple transmitters or multiple receivers on wireless power transfer," *IEEE Trans. Ind. Electron.*, vol. 60, no. 7, pp. 2602–2613, Jul. 2013.

[8] K. Lee and D.-H. Cho, "Diversity analysis of multiple transmitters in wireless power transfer system," *IEEE Trans. Magn.*, vol. 49, no. 6, pp. 2946–2952, Jun. 2013.

[9] B. L. Cannon, J. F. Hoburg, D. D. Stancil, and S. C. Goldstein, "Magnetic resonant coupling as a potential means for wireless power transfer to multiple small receivers," *IEEE Trans. Power Electron.*, vol. 24, no. 7, pp. 1819–1825, Jul. 2009.

[10] U. Azad and I. Tzanidis, "Resonant coupling efficiency limits for multiple receivers in a wireless power transfer system," in *Proc. IEEE Int. Symp. Antennas Propag. Soc.*, 2013, pp. 846–847.

[11] J. Kim, H.-C. Son, D.-H. Kim, and Y.-J. Park, "Impedance matching considering cross coupling for wireless power transfer to multiple receivers," in *Proc. IEEE Wireless Power Transfer Conf.*, 2013, pp. 226–229.

[12] D. Ahn and S. Hong, "Effect of coupling between multiple transmitters or multiple receivers on wireless power transfer," *IEEE Trans. Ind. Electron.*, vol. 60, no. 7, pp. 2602–2613, Jul. 2013.

[13] C. K. Lee, W. X. Zhong, and S. Y. R. Hui, "Effects of magnetic coupling of non-adjacent resonators on wireless power domino-resonator systems," *IEEE Trans. Power Electron.*, vol. 27, no. 4, pp. 1905–1916, Apr. 2012.

[14] T. Deyle and M. Reynolds, "Surface based wireless power transmission and bidirectional communication for autonomous robot swarms," in *Proc. IEEE Int. Conf. Robot. Autom.*, 2008, pp. 1036–1041.

[15] W. X. Zhong and S. Y. R. Hui, "Auxiliary circuits for selection and enhancement of multi-frequency wireless power transfer to multiple loads," Patent PCT/CN2014/078414, May 26, 2014.

[16] X. Liu, "Inductive power transfer using a relay coil," U.S. Patent 13/907 483, May 31, 2013.

[17] W. X. Zhong, C. Zhang, X. Liu, and S. Y. R. Hui, "A methodology for making a 3-coil wireless power transfer system more energy efficient than a 2-coil counterpart for extended transmission distance," *IEEE Trans. Power Electron.*, vol. 30, no. 2, pp. 933–942, Oct. 2014 .

Wenxing Zhong (M'13) was born in China, in 1984. He received the B.S. degree in electrical engineering from Tsinghua University, Beijing, China, in 2007, and the Ph.D. degree from the City University of Hong Kong, Kowloon, Hong Kong, in 2012.

He is currently a Postdoctoral Research Fellow in the Department of Electrical and Electronic Engineering, The University of Hong Kong, Pokfulam, Hong Kong. His current research interests include wireless power transfer and power electronics.

S. Y. R. Hui (M'87–SM'94–F'03) received the B.Sc. (Eng. Hons.) degree from the University of Birmingham, Birmingham, U.K., in 1984, and the D.I.C. and Ph.D. degrees from Imperial College London, London, U.K., in 1987.

He is currently the holder of the Philip Wong Wilson Wong Chair Professorship at the University of Hong Kong, Pokfulam, Hong Kong. Since July 2010, he has concurrently held a part-time Chair Professorship of Power Electronics at Imperial College London. He has published more than 300 technical papers, including more than 180 refereed journal publications and book chapters. More than 55 of his patents have been adopted by industry. His inventions underpin key dimensions of Qi, the world's first wireless power standard, with freedom of positioning and localized charging features for wireless charging of consumer electronics. He is an Editor for the IEEE Journal of Emerging and Selected Topics in Power Electronics. He is an Associate Editor for the IEEE Transactions on Power Electronics and the IEEE Transactions on Industrial Electronics.

Dr. Hui received the IEEE Rudolf Chope R&D Award from the IEEE Industrial Electronics Society and the IET Achievement Medal (The Crompton Medal), in 2010. He is the recipient of the 2015 IEEE William E. Newell Power Electronics Award. He is a Fellow of the Australian Academy of Technological Sciences and Engineering.